The Shear Lag Problem in Structure Analysis: Fundamentals, Methods and Applications

João Manuel Correia[1] and Nuno Domingues[2]

***Abstract*—**Most engineering problems involving beam-like structural elements are approximations to the structural problem involving plates connected by connectors to metal beams. Technical standards define some parameters (such as effective width), but most technical standards only consider the parameters of span length and distance between adjacent beams. Numerical and experimental works found in the literature show that this effective width depends on several other parameters, such as the width and thickness of the concrete slab and the type of loading.

Shear lag effect is an unexpected major phenomenon that controls the design of tall buildings using framed tube system. There is much research with different analysis methods have been conducted to study the effect of shear lag not only in box girder, but also in tube structures.

The present paper focus on the additional weight of solar energy systems on roofs and platforms. These structures weren't design and calculated for this additional weight thereby its behaviour should be known.

***Index Terms*—** Shear Lag, Effects, Steel Tension, Tube Structural Systems, Tall Buildings.

I. Introduction

Occurrence of shear lag in buildings is reported in the literature for several years ago and all over the world [1-8], but explanation of its origin and comprehensive studies of it are lacking. Historically, the problem of Shear Lag effects was first approached by Von Karmen and successively by several authors. Building suffers from shear lag effects which cause a nonlinear distribution of axial stresses along the face of the building. Major advancements in structural engineering have been the development of different structural systems that allow for higher buildings. As the height of the building increase, the lateral resisting system becomes more important than the structural system that resists the gravitational loads. Also, introducing renewable energy systems at the top of building cause an extra height (such as solar systems) and vibrations (such as wind power) that affect the structure equilibrium that was firstly designed.

The need to consider the effects of Shear Lag in the design of structures initially arose in the field of aeronautical engineering [9-14] but immediately naval architects [15-17] and civil engineers [18-19] were faced with the need to address the same problem.

However, only in 1990 a methodical study [20] allowed the identification of parameters that governs the effects of the phenomenon on the behaviour of wide-beam beams. The results of the studies were used as the basis for the wide chord design rules included in the most recent international legislation.

The objective of the present paper is to present the calculation structure using shear lag. Shear lag is a concept used to explain uneven tension distribution in connected elements. Further conclusions can be made for renewable energy systems decentralization on the top of the buildings.

II. Discretization of Structural Models

For the study, authors intend to use a refined mesh, whenever possible with elements similar to a square and that respect the applicability conditions of the models used in order to be led to good analytical results.

For the present study, 3 types of models are used. The first two models were developed to reproduce wall elements by bar elements and the third one is a plate model.

- The 1st Model is based only on the axial deformability of the section
- The 2nd Model considers the deformability of the section by shear, by bending and axial
- The 3rd Model is a plate model, using the finite element formulation.

A. 1st Model

In this model it is deduced by reproducing the axial deformability of wall elements with bar elements: Both the bending deformability and the shear deformability do not enter the mathematical deduction of the model.

The bar model itself, through its geometric characteristics obtained based on the axial deformability of a plate element, defines areas and inertia that give rise to these two types of deformability. The shear deformability itself is intrinsically linked to the global model, and it is to be expected that when it assumes an important value, as in the case of low-rise buildings (2 and 4 store models). This model departs from the theory of Strength of Materials and is illustrated in Figure 1.

[1]Lusopratica Lda, Rua D. Jerónimo, Cascais, Portugal

[2]Instituto Politécnico de Lisboa/ Instituto Superior de Engenharia de Lisboa, Rua Conselheiro Emidio Navarro, 1, 1959-007 Lisbon, Portugal

https://doi.org/10.17758/EARES12.UH0423101

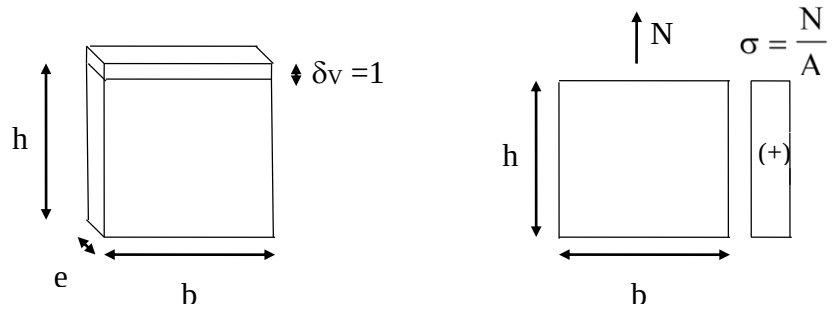

Fig. 1 - Applying a unit vertical displacement to a plate element

From Hooke's Law, σ = ε E, and

$$\delta_V = \int_0^h \varepsilon \ \ dx_3,$$

one gets the following relation,

$$\delta_V = \int_0^h \frac{\sigma}{E}\, dx_3 = \int_0^h \frac{N}{EA}\, dx_3 = \frac{N \times h}{E \times A} \qquad (1)$$

As a unit displacement δV was applied, one gets:

$$1 = \frac{N \times h}{E \times A} \Leftrightarrow N = \frac{E \times A}{h}$$

where A is the cross-sectional area of the wall element, i.e. A = b e, E the modulus of elasticity and h the height of the element.

Reproducing the same wall element with bar elements, the model illustrated in Figure 2 is obtained.

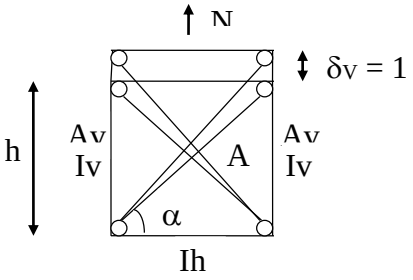

Fig. 2 – First model application

Knowing the relationship for a wall element, $N = \frac{E\,A}{h} = \frac{E \times b \times e}{h}$, in each bar the following relationship between the diagonals and the vertical bars is obtained:

$$\frac{2Av}{h} + \frac{2Ad \sin^3 \alpha}{h} = \frac{b\,e}{h} \Leftrightarrow Av + Ad \sin^3 \alpha = \frac{b\,e}{2}$$

$$\begin{cases} Av + Ad \sin^3 \alpha = \dfrac{b\,e}{2} & (2) \\ Av = 3Ad & (3) \end{cases}$$

In this formulation it was assumed that Av = 3 Ad which imposes the following relations between the sides of the element:

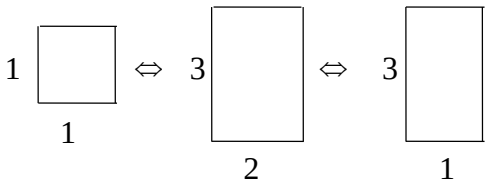

Fig. 3 – First model sides unit relations

Developing expressions (2) and (3) we obtain the relationship of the areas of the vertical bars and the diagonals with the base wall element, allowing the calculation of the diagonals (Ad):

$$3\,Ad + Ad \sin^3 \alpha = \frac{b\,e}{2} \Leftrightarrow Ad\,(3 + \sin^3 \alpha) = \frac{b\,e}{2} \Leftrightarrow Ad = \frac{b\,e}{2\,(3 + \sin^3 \alpha)}$$

$$Ad = \frac{b\,e}{6 + 2 \sin^3 \alpha} \qquad (4)$$

The calculation of the area of the columns (Ad) is obtained by replacing (4) in (3):

$$Av = 3\,Ad = 3 \times \frac{b\,e}{6 + 2 \sin^3 \alpha} = \frac{3\,b\,e}{6 + 2 \sin^3 \alpha} = \frac{b\,e}{2 + \frac{2}{3} \sin^3 \alpha} \qquad (5)$$

Taking Figure 4 as a reference, it is possible to obtain the areas and moments of inertia for the various elements. The vertical elements (pillars) are intended to reproduce the mechanical characteristics of the wall, the diagonals functioning as struts. Each Column reproduces half the width of the wall (b/2) while maintaining the height (h) and thickness (e). Diagonals are only assigned an area (4).

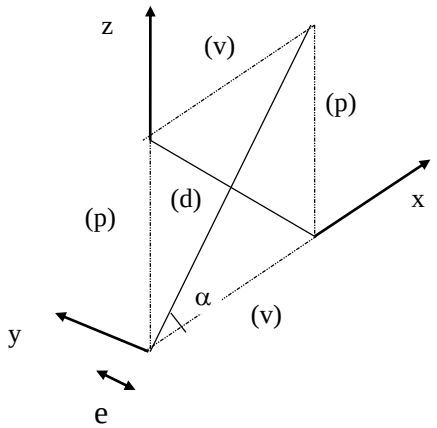

Fig. 4 - Model of bars

Expressions (4) and (5) were deduced solely based on the axial deformation of a wall element. In addition to the areas, the inertias in their bending planes are assigned to the vertical and horizontal bars:

$$I_x^{(p)} = \frac{\frac{b}{2}\times e^3}{12} = \frac{b\,e}{12}(6);\ I_y^{(p)} = \frac{e(\frac{b}{2})^3}{12} = \frac{e\,b^3}{2^3\times 12} = \frac{e\,b^3}{96}(7)$$

$$A^{(p)} = \frac{3\,b\,e}{6+2\sin^3\alpha}(5);\ I_y^{(v)} = \frac{e(\frac{h}{2})^3}{12} = \frac{e\,h^3}{2^3\times 12} = \frac{e\,h^3}{96}(8)$$

$$I_z^{(v)} = \frac{\frac{h}{2}\times e^3}{12} = \frac{h\,e^3}{2\times 12} = \frac{h\,e^3}{24}(9);\ A^{(v)} = \frac{e\,h}{2}(10);\ A^{(d)} = \frac{b\,e}{6+2\sin^3\alpha}(4)$$

B. 2nd Model - Model of connecting struts (rods) and columns

This model intends to simulate the load-bearing walls using struts and uprights as illustrated in Figure 5.

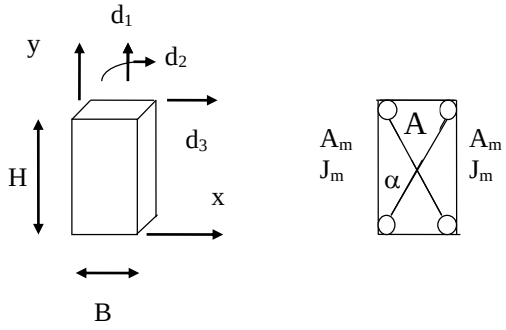

Fig. 5 - Model of connecting struts and tie rods

To simulate the areas of rigid struts (Am) and areas of Tie Rods (Am). With this aim, we consider the three independent displacements as indicated in the figure and determine stiffness matrices for both for the rigid wall and for the connecting struts rod and tie rod system.

The torsion factors are used to consider the uniform torsion of the wall, taking the value of:

$$J_m = \frac{B/2\,t^3}{3}$$

The inertia of the cross section for bending outside the plane of the wall must also be taken into account in the tie rods, the value of this inertia being the following:

$$I_m^{\text{fora plano}} = \frac{B}{2}\times\frac{t^3}{12}$$

To obtain the Wall Stiffness Matrix (Plate) the displacement fields, the deformation fields and the stress fields installed on the plate are calculated. The displacement fields for each of the independent displacements are those indicated in the following table, representing u the displacement according to x and v the displacement according to y, as shown in Table 1.

TABLE I: Displacement fields installed on the plate for independent displacements

Displacement	u	v
1	0	$\frac{y}{H}$
2	0	$\frac{B-2x}{H}\times\frac{y}{2}$
3	$\frac{y}{H}$	0

The associated deformation fields are:

$$\varepsilon_{xx} = \frac{\partial_u}{\partial_x} \qquad \varepsilon_{yy} = \frac{\partial_v}{\partial_y} \qquad \gamma_{xy} = \frac{\partial_u}{\partial_y} + \frac{\partial_v}{\partial_x}$$

and are listed in Table 2.

TABLE II: Deformation fields installed on the plate for independent displacements

Displacement	ε_{xx}	ε_{yy}	γ_{xy}
1	0	$\frac{1}{H}$	0
2	0	$\frac{B-2x}{2H}$	$-\frac{y}{H}$
3	0	0	$\frac{1}{H}$

The stress fields associated with these displacement, for a plane stress state, are given by:

$$\begin{bmatrix}\sigma_{xx}\\ \sigma_{yy}\\ \sigma_{xy}\end{bmatrix} = \frac{E}{1-\nu^2}\times\begin{bmatrix}1 & \nu & 0\\ \nu & 1 & 0\\ 0 & 0 & \frac{1-\nu}{2}\end{bmatrix}\times\begin{bmatrix}\varepsilon_{xx}\\ \varepsilon_{yy}\\ \gamma_{xy}\end{bmatrix}$$

and are shown in Table 3.

TABLE III - Stress fields installed on the plate for independent displacements

Displacement	σ_{xx}	σ_{yy}	σ_{xy}
1	$\frac{E}{1-\nu^2}\frac{\nu}{H}$	$\frac{E}{1-\nu^2}\frac{1}{H}$	0
2	$\frac{E\nu}{1-\nu^2}\frac{B-2x}{2H}$	$\frac{E}{1-\nu^2}\frac{B-2x}{2H}$	$-\frac{E}{1-\nu^2}\times\frac{1-\nu}{2}\times\frac{y}{H}$
3	0	0	$\frac{E}{1-\nu^2}\times\frac{1-\nu}{2}\times\frac{1}{H}$

The stiffness matrix associated with the chosen independent displacements are given by:

$$K_{ij} = \iiint_V \sigma_{\alpha\beta}^{(j)}\times\varepsilon_{\alpha\beta}^{(i)}\,dV$$

In the notation indicated it is used the Einstein sum convention, having in addition $\gamma_{xy} = 2\varepsilon_{xy}$.

Carrying out the integrations, the following stiffness matrix is obtained:

$$[K] = \frac{Et}{1-\nu^2} \times \begin{bmatrix} \frac{B}{H} & 0 & 0 \\ 0 & \frac{B^3}{12H} + BH \times \frac{1-\nu}{6} & -\frac{1-\nu}{2} \times \frac{B}{2} \\ 0 & -\frac{1-\nu}{2} \times \frac{B}{2} & \frac{1-\nu}{2} \times \frac{B}{H} \end{bmatrix}$$

The determination of the stiffness matrix of this model follows the principles used previously. For illustrative purposes, the schematic deformations for the three displacements in Figure 6 are indicated. Table 4 shows the forces installed in the elements, for independent displacements.

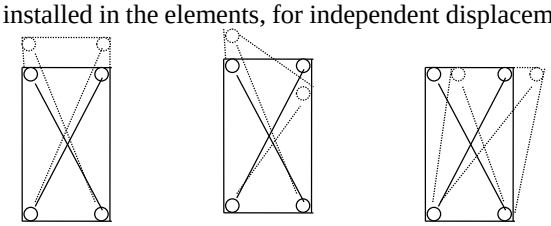

Fig 6 - Deformed models of struts and columns for independent displacements

TABLE IV - Efforts on the struts and struts model elements for unit independent displacements

Displacement	Left connecting Strut Rod	Right connecting Strut Rod	Left Column	Right Column
1	$\frac{EA_b}{H}\cos^2\alpha$	$\frac{EA_b}{H}\cos^2\alpha$	$\frac{EA_m}{H}$	$\frac{EA_m}{H}$
2	$\frac{EA_b}{H} \times \frac{B}{2}\cos^2\alpha$	$-\frac{EA_b}{H} \times \frac{B}{2}\cos^2\alpha$	$\frac{EA_m}{H} \times \frac{B}{2}$	$-\frac{EA_m}{H} \times \frac{B}{2}$
3	$-\frac{EA_b}{H}\sin\alpha\cos\alpha$	$\frac{EA_b}{H}\sin\alpha\cos\alpha$	0	0

The associated stiffness matrix is:

$$[K] = \begin{bmatrix} 2\frac{EA_m}{H} + 2\frac{EA_b}{H}\cos^3\alpha & 0 & 0 \\ 0 & 2\frac{EA_m}{H} \times \frac{B^2}{4} + 2\frac{EA_b}{H} \times \frac{B^2}{4}\cos^3\alpha & -2\frac{EA_b}{H} \times \frac{B}{2}\cos^2\alpha\sin\alpha \\ 0 & -2\frac{EA_b}{H} \times \frac{B}{2}\cos^2\alpha\sin^2\alpha & 2\frac{EA_b}{H}\cos\alpha\sin^2\alpha \end{bmatrix}$$

C. Determining the areas of connecting strut rods and columns

The determination of the areas of the different elements is achieved by equating the different terms of the calculated stiffness matrices. They are obtained like this:

$$\frac{E_t}{1-\nu^2} \times \frac{B}{H} = 2 \times \frac{E}{H} \times (A_m + A_b\cos^3\alpha)$$

(Axial Load, K_{11})

$$\frac{E_t}{1-\nu^2} \times \left[\frac{B^3}{12H} + BH \times \frac{1-\nu}{6}\right] = 2 \times \frac{E}{H} \times \frac{B^2}{4} \times (A_m + A_b\cos^3\alpha)$$

(Simple Bending, K_{22})

$$\frac{E_t}{1-\nu^2} \times \frac{1-\nu}{2} \times \frac{B}{H} = 2 \times \frac{E}{H} \times A_b\sin^2\alpha\cos\alpha$$

(Shear Force, K_{33})

$$\frac{E_t}{1-\nu^2} \times \frac{1-\nu}{2} \times \frac{B}{2} = 2 \times \frac{E}{H} \times A_b \times B \times \cos^2\alpha\sin\alpha$$

(Cross term Flexion – Shear/Cut, K_{23})

The term relating to the shear effect directly provides the area to be considered on the connecting strut rods, obtaining the following expression:

$$A_b = \frac{B_t}{4 \times (1+\nu)} \times \frac{1}{\sin^2\alpha\cos\alpha}$$

The cross term between bending and shearing also gives the area of the connecting strut rods, obtaining the following expression:

$$A_b = \frac{H_t}{4 \times (1+\nu)} \times \frac{1}{\cos^2\alpha\sin\alpha}$$

These two expressions are identical in every way, it is sufficient to comply with the definition of the angle α:

$$tg\alpha = \frac{B}{H}$$

The area of the connecting strut rods can be rewritten as follows

$$A_b = \frac{1}{4\times(1+\nu)} \times \frac{(H^2+B^2)^{3/2}}{BH}$$

The equations relating to axial forces and bending are linearly independent, obtaining a relationship between width and length so that the system of equations is possible:

$$\frac{\frac{B^3}{12H} + BH \times \frac{1-\nu}{6}}{\frac{B}{H}} = \frac{B^2}{4} \qquad \rho = \frac{B}{H}$$

$$\rho^2 - (1-\nu) = 0$$

This quadratic equation gives only one real root with physical meaning:

$$\rho = \sqrt{1-\nu}$$

With current values of Poisson's ratio, there are relationships between the base of the wall and its height from 0.9 to 1.0. The area of the columns is determined using, for example, the equation relating to the axial force:

$$A_m = \frac{Bt}{2(1-\nu^2)} - A_b \cos^3\alpha$$

$$A_m = \frac{Bt}{2(1-\nu^2)} - \frac{t}{4(1+\nu)} \frac{(H^2+B^2)^{3/2}}{BH} \times \frac{H^3}{(H^2+B^2)^{3/2}}$$

$$A_m = \frac{Bt}{2(1-\nu^2)} - \frac{t}{4(1+\nu)} \times \frac{H^2}{B} = \frac{2B^2 - H^2(1-\nu)}{4B(1-\nu^2)} t$$

$$A_m = \frac{2B^2 - H^2(1-\nu)}{4B(1-\nu^2)} t$$

In order for the column area to be positive, it is necessary to obtain the following relationship:

$$2B^2 > H^2(1-\nu) \qquad \frac{B}{H} > \sqrt{\frac{1-\nu}{2}}$$

The most current values that can be established for this relationship vary from 0.71 (considering a null Poisson Coefficient) to 0.63 (Poisson Coefficient equal to 0.2). It is usual practice not to consider the Poisson Ratio in this type of approach, obtaining the following relationships for the following areas of the structural elements:

$$\rho = 1 \times 1 = 1$$

$$A_b = \frac{t}{4} \times \frac{(H^2+B^2)^{3/2}}{BH}$$

$$A_m = \frac{2B^2 - H^2}{4B} t$$

It is important to know the limitations regarding the shape of the wall element, which must obey the following inequality:

$$\frac{1}{\sqrt{2}} < \frac{B}{H}$$

One can thus summarize the relations presented above to the following two:

$$A_b = \frac{t}{4} \times \frac{\left(H^2+B^2\right)^{\frac{3}{2}}}{BH} \qquad A_m = \frac{2B^2 - H^2}{4B} t$$

For H=B=0.75 $\Rightarrow$ A_b = 0.106066 m^2; A_m = 0.0375 m^2.

Limitation to model dimensions $\frac{1}{\sqrt{2}} < \frac{B}{H}$ is satisfied.

Results

For calculation, elements measuring 0.75 m by 0.75 m were used and shown in Figure 7.

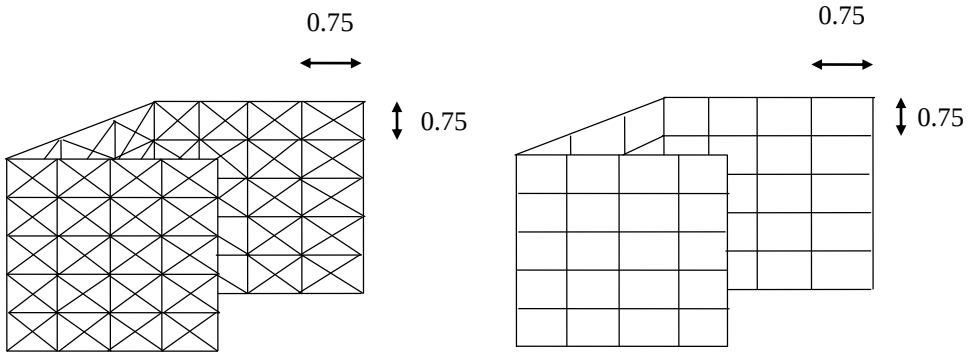

Fig. 7 - Modelling of wall elements by bar elements and by plate elements

For a mesh of 0.75×0.75:

b=h=0.75$\Rightarrow$ $\operatorname{tg}\alpha = \frac{0.75}{0.75} = 1 \Rightarrow \alpha = 1$

$$I_x^{(p)} = \frac{0.75 \times 0.2^3}{24} = 0.00025\ \text{m}^4 \quad ;$$

$$I_y^{(p)} = \frac{0.2 \times 0.75^3}{96} = 8.7890625 \times 10^{-4}\ \text{m}^4$$

$$A^{(p)} = \frac{3 \times 0.75 \times 0.2}{6 + 2\sin 45^{o\ 3}} = 6.709301263 \times 10^{-2}\ m^2 \qquad A^{(v)} = \frac{0.2 \times 0.75}{2} = 0.075\ m^2 \quad ;$$

$$A^{(d)} = \frac{0.75 \times 0.2}{6 + 2\sin 45^{0\ 3}} = 2.236433754 \times 10^{-2}\ m^2$$

$$I_y^{(v)} = \frac{0.2 \times 0.75^3}{96} = 8.7890625 \times 10^{-4}\ m^4 ;$$

$$I_z^{(v)} = \frac{0.75 \times 0.2^3}{24} = 0.00025\ m^4$$

In this modelling, the axial rigidity of the wall is maintained. This modelling reproduces a wall element with bar elements. The non-consideration of flat sections leads to a decrease in the model's rigidity.

1ºMod	2 floors (displacements at the top)		4 floors (displacements at the top)		8 floors (displacements at the top)	
	λ = δ R.M. N/Shear Def. / δ S.A.P.	λ = δ R.M. Y/Shear Def. / δ S.A.P.	λ = δ R.M. N/Shear Def. / δ S.A.P.	λ = δ R.M. Y/Shear Def. / δ S.A.P.	λ = δ R.M. N/Shear Def. / δ S.A.P.	λ = δ R.M. Y/Shear Def. / δ S.A.P.
	0,238240059	0,671982636	0,549245067	0,79923553	0,912896092	1,016772909
	0,234750451	0,809769787	0,496905338	0,801196742	0,806292317	0,929730225
	0,382763226	1,381149601	0,6744421	1,114239969	0,908128982	1,056174749

1ºMod	12 floors (displacements at the top)		16 floors (displacements at the top)	
	λ = δ R.M. N/Shear Def. / δ S.A.P.	λ = δ R.M.Y/Shear Def. / δ S.A.P.	λ = δ R.M. N/Shear Def. / δ S.A.P.	λ = δ R.M. Y/Shear Def. / δ S.A.P.
	1,029572812	1,081640924	1,07128685	1,101761805
	0,930790253	0,994122565	0,986042483	1,023781594
	0,925627282	0,992693232	0,984149454	1,024259164

TABLE I - Table of Horizontal Displacements for the 1st Model

2ºMod	2 floors (displacements at the top)		4 floors (displacements at the top)		8 floors (displacements at the top)	
	λ = δ R.M. N/Shear Def. / δ S.A.P.	λ = δ R.M. Y/Shear Def. / δ S.A.P.	λ = δ R.M. N/Shear Def. / δ S.A.P.	λ = δ R.M. Y/Shear Def. / δ S.A.P.	λ = δ R.M. N/Shear Def. / δ S.A.P.	λ = δ R.M. Y/Shear Def. / δ S.A.P.
	0,392105816	1,10597815	0,748598351	1,089325031	0,945027524	1,052560519
	0,347811618	1,199773371	0,663595451	1,069963377	0,876288856	1,010442761
	0,279227621	1,007555302	0,535698776	0,885023321	0,815948715	0,948966993

2ºMod	12 floors (displacements at the top)		16 floors (displacements at the top)	
	λ = δ R.M. N/Shear Def. / δ S.A.P.	λ = δ R.M. Y/Shear Def. / δ S.A.P.	λ = δ R.M. N/Shear Def. / δ S.A.P.	λ = δ R.M. Y/Shear Def. / δ S.A.P.
	1,000809141	1,051422601	1,022105036	1,051180913
	0,944224984	1,008471414	0,975300891	1,012628885
	0,972435293	1,0428927	0,997238817	1,037881994

Table II - Table of Horizontal Displacements for the 2nd Model

3ºMod	2 floors (displacements at the top)		4 floors (displacements at the top)		8 floors (displacements at the top)	
	λ = δ R.M. N/Shear Def. / δ S.A.P.	λ = δ R.M. Y/Shear Def. / δ S.A.P.	λ = δ R.M. N/Shear Def. / δ S.A.P.	λ = δ R.M. Y/Shear Def. / δ S.A.P.	λ = δ R.M. N/Shear Def. / δ S.A.P.	λ = δ R.M. Y/Shear Def. / δ S.A.P.
	0,353311194	0,996553596	0,709155635	1,031929851	0,961735193	1,071169324
	0,317340769	1,094664426	0,636009942	1,025485248	0,915620088	1,05579534
	0,355062268	1,281194424	0,650823505	1,075219893	0,914670873	1,063783117

Table III - Table of Horizontal Displacements for the 3rd Model

3ºMod	12 floors (displacements at the top)		16 floors (displacements at the top)	
	λ = δ R.M. N/Shear Def. / δ S.A.P.	λ = δ R.M.Y/Shear Def. / δ S.A.P.	λ = δ R.M. N/Shear Def. / δ S.A.P.	λ = δ R.M. Y/Shear Def. / δ S.A.P.
	1,032528278	1,084745856	1,063859862	1,09412354
	1,005867788	1,074308483	1,045672767	1,085694126
	1,003775748	1,076503914	1,043770047	1,086309636

λ - Relation between the horizontal displacements obtained from the Strength of Materials and those obtained by the 3 models under analysis using the SAP2000 calculation program.

The parameter λ could be a good indicator between the theory of Strength of Materials, which considers the flat sections after deforming, and the proposed models that essentially intend to show the differences between the sections obtained by the theory of Strength of Materials and the sections that are obtained with each of the formulations presented.

From here it can be concluded when it is important to consider the Shear Lag effect, that is, the fact that we approach or distance ourselves from the flat sections and which are the various effects directly linked.

Almost all models correctly translate the various deformities with the exception of the 1st Mod. for the reasons already described above. Obviously, as we increase in height and the deformability by shear is no longer important, this model begins to approach the others as well as the theory of Strength of Materials itself.

The parameter λ indicates us in the idealized model to simulate the shear wall Section when using a certain type of model, we begin to move away from the linearity of the sections. This factor may be important as it is a good indicator of errors, we are making regarding the theory that sections remain flat after deforming.

The fact that the parameter λ moving away or approaching 1 indicates the greater or lesser flexibility of the section.

Parameter indicating the approximation of vertical displacements obtained by the models described to the theory of Resistance of Materials

TABLE IV - Relationship between areas of vertical displacement diagrams obtained by the models described and by the Strength of Materials for 2 floors

	2 floors (displacements at the top)		
	λ = δ SAP2000 (1ºMod) - RM / δ RM	λ = δ SAP2000 (2ºMod) - RM / δ RM	λ = δ SAP2000 (3ºMod) - RM / δ RM
	0,278119471	0,161154407	0,178152746
	0,421644423	0,347348567	0,385621204
	0,412667506	0,408695027	0,436692248

TABLE V- Relationship between areas of vertical displacement diagrams obtained by the models described and by the Strength of Materials for 4 floors

4 floors (displacements at the top)			
	$\lambda = \frac{\delta \text{ SAP2000 (1ºMod) - RM}}{\delta \text{ RM}}$	$\lambda = \frac{\delta \text{ SAP200 (2ºMod) - RM}}{\delta \text{ RM}}$	$\lambda = \frac{\delta \text{ SAP2000 (3ºMod) - RM}}{\delta \text{ RM}}$
	0,085438123	0,075306201	0,079762681
	0,208860242	0,117119126	0,143937157
	0,256095202	0,167402449	0,198502199

TABLE VI - Relationship between areas of vertical displacement diagrams obtained by the models described and by the Strength of Materials for 8 floors

8 floors (displacements at the top)			
	$\lambda = \frac{\delta \text{ SAP2000 (1ºMod) - RM}}{\delta \text{ RM}}$	$\lambda = \frac{\delta \text{ SAP2000 (2ºMod) - RM}}{\delta \text{ RM}}$	$\lambda = \frac{\delta \text{ SAP2000 (3ºMod) - RM}}{\delta \text{ RM}}$
	0,12649386	0,055577265	0,082795592
	0,076859581	0,045828261	0,089067749
	0,104111953	0,069035691	0,104635137

TABLE VII - Relationship between areas of vertical displacement diagrams obtained by the models described and by the Strength of Materials for 12 floors

12 floors (displacements at the top)			
	$\lambda = \frac{\delta \text{ SAP2000 (1ºMod) - RM}}{\delta \text{ RM}}$	$\lambda = \frac{\delta \text{ SAP2000 (2ºMod) - RM}}{\delta \text{ RM}}$	$\lambda = \frac{\delta \text{ SAP2000 (3ºMod) - RM}}{\delta \text{ RM}}$
	0,120311169	0,05359803	0,084576801
	0,069969337	0,036709153	0,086960417
	0,081040935	0,050432304	0,093967488

TABLE VIII - Relationship between areas of vertical displacement diagrams obtained by the models described and by the Strength of Materials for 16 floors

16 floors (displacements at the top)			
	$\lambda = \frac{\delta \text{ SAP2000 (1ºMod) - RM}}{\delta \text{ RM}}$	$\lambda = \frac{\delta \text{ SAP2000 (2ºMod) - RM}}{\delta \text{ RM}}$	$\lambda = \frac{\delta \text{ SAP2000 (3ºMod) - RM}}{\delta \text{ RM}}$
	0,110617655	0,052148998	0,088165015
	0,067403684	0,029273879	0,088421207
	0,072851125	0,046047483	0,092225179

These values are obtained by direct integration of the area diagrams of displacements for each situation.

This parameter may be indicative of the approximation between the models presented and the theory of Strength of Materials that considers flat sections.

III. Conclusion

From the analysis of the 3 proposed models, it was concluded that for lower levels and mainly for sections with Flanged Sections Shear Wall, almost forming a rectangle, there is a strong warping (flexural torsional buckling) effect on these walls, with the remaining sections showing a reasonable approximation of the theory of Strength of Materials, although for low levels the Shear Lag effect becomes important although it dissipates. this effect quickly in height. (Roughly at 8 levels this effect is practically no longer felt). The parameter defined in two ways clearly indicates that the Shear-Lag is important for low floors. We can analyze the numerous results presented so far both graphically and analytically that we are directly or indirectly led to the same conclusion.

References

[1] Moffat, K.R., and Dowling, P.J. Steel box girders, parametric study on the Shear Lag phenomenon in Steel box girder bridges. CESLIC Report BG17. Engineering Structures Laboratories, Imperial College of Science and Technology, London, 1972.

[2] BIS (1987) IS 875 (Part 3)—1987 Indian standard code of practice for design loads (other than earthquake) for buildings and structures. Bureau of Indian Standard, New Delhi

[3] Moffat, K.R. and Dowling, P.J. Shear Lag in Steel box girder bridges. The Structural Engineer, vol 53, October 1975.

[4] Coull, A. and Stafford Smith, B., Tall Building Structures: Analysis and Design, John Wiley & Sons, New York, 1991. Designbuild-Network

[5] Bauer, K., and Kristek, V., Stress Distribution In Front Columns of High-Rise Buildings, Journal of Structural Engineering, Vol. 119, No. 5, May, 1993. Chicago Architect Foundation https://doi.org/10.1061/(ASCE)0733-9445(1993)119:5(1464)

[6] Kwan, A. K. H., Simple Method for Approximate Analysis of Framed Tube Structures, Journal of Structural Engineering, Vol. 120, No. 4, April, 1994. https://doi.org/10.1061/(ASCE)0733-9445(1994)120:4(1221)

[7] Nagpal, A. K. and Singh, Y., Negative Shear Lag in Framed-Tube Buildings, Journal of Structural Engineering, Vol. 120, No. 11, November, 1994. https://doi.org/10.1061/(ASCE)0733-9445(1994)120:11(3105)

[8] Kwan, A. K. H., Shear Lag in Shear/Core Walls, Journal of Structural Engineering, Vol. 122, No. 9, September, 1996. https://doi.org/10.1061/(ASCE)0733-9445(1996)122:9(1097)

[9] Visnjic, G., Nožak, D., Kosel, F. and Kosel, T. (2014), "Reducing shear-lag in thin-walled composite I-beam wing spars", Aircraft Engineering and Aerospace Technology, Vol. 86 No. 2, pp. 89-98. https://doi.org/10.1108/AEAT-09-2012-0153

[10] Eric Reissner, Least Work Solutions of Shear Lag Problems, 30 Aug 2012, https://doi.org/10.2514/8.10712

[11] Martin Goland, Shear Lag Solutions for Sheet-Stringer Panels by Means of a Hydrodynamic Analogy, Journal of the Aerospace Sciences, 2012

[12] Giola Santoni-Bottai, Exact Shear-Lag Solution for Guided Waves Tuning with Piezoelectric-Wafer Active Sensors, AIAA Journal, 2012 https://doi.org/10.2514/1.J050667

[13] John de S. Coutinho, A Practical Method of Allowance for Shear Lag, Journal of the Aeronautical Sciences, 2012

[14] S. B. Batdorf, Use of shear lag for composite microstress analysis rectangular array, AIAA Journal, 2012

[15] Sisi Xiang, Tuning the deformation mechanisms of boron carbide via silicon doping, Sci Adv, 2019 https://doi.org/10.1126/sciadv.aay0352

[16] Xulong QIN, A Study on The Boundary Layer for The Planar Magnetohydrodynamics System, Selections from Acta Mathematica Scientia, 2015

[17] S. B. Batdorf, Note on Shear Interaction between Two Fibers. Technical rept., 1982-09-01, California Univ Los Angeles School of Engineering And Applied Science

[18] A. K. H. Kwan, Shear Lag in Shear/Core Walls, Univ. of Hong Kong, Pokfulum Rd., Hong Kong. Journal of Structural Engineering, Vol. 122, Issue 9 (September 1996), https://doi.org/10.1061/(ASCE)0733-9445(1996)122:9(1097)

[19] Q. Z. Luo, Q. S. Li, J. Tang, Shear Lag in Box Girder Bridges, August 15, 2002, https://doi.org/10.1061/(ASCE)1084-0702(2002)7:5(308)

[20] B.A. Burgan, P.J. Dowling, The treatment of shear lag in design, Thin-Walled Structures, Volume 9, Issues 1–4, 1990, Pages 121-134, ISSN 0263-8231, https://doi.org/10.1016/0263-8231(90)90041-V